A tear-based battery charged by biofuel for smart contact lenses

[1]Jeonghun Yun^, [1]Zongkang Li^, [2]Xinwen Miao, [1]Xiaoya Li, [3]Jaeyoon Lee, [2]Wenting Zhao, [1,3]Seok Woo Lee*

[1]School of Electrical and Electronic Engineering, Nanyang Technological University, Singapore 639798, Singapore

[2]School of Chemistry, Chemical Engineering and Biotechnology, Nanyang Technological University, Singapore 639798, Singapore

[3]Rolls-Royce@NTU Corporate Lab, Nanyang Technological University, Singapore 639798, Singapore

*Corresponding author: sw.lee@ntu.edu.sg

^equally contributed

Abstract

Smart contact lenses developed for medical and personal applications will require miniaturized power supplies, with integrated batteries providing promising options. However, charging batteries in small wearable devices is challenging because it is difficult to transfer electrical power through a miniaturized wired connection or wireless transmission unit. Herein, we develop safe, tear-based batteries integrated into contact lenses that are charged by biofuel during their storage. Enzymatic reactions of glucose oxidase and self-reduction of conducting polymer are utilized to charge the cathode and anode, respectively. The electrodes are embedded into a contact lens and discharged in an artificial tear solution followed by charging in a glucose solution via a bio-reaction (called bio-charging). The bio-charging battery shows

a discharging capacity of 45 μA cm^{-2} and a maximum power of 201 μW cm^{-2}, with its performance verified over 15 cycles. The bio-chargeable battery can also be charged conventionally by an external power supply.

Keyword

batteries, biofuel, smart contact lenses, glucose oxidase, self-reduction

1. Introduction

Smart contact lenses are wearable devices that promise to provide wearers with both medical diagnostics and personal applications and are typically composed of sensors, wireless communicators, actuators, and power supplies [1-6]. The development of the power supply for smart contact lenses has focused on providing power through either inductive power transmission [3, 7-10], supercapacitors [11], biofuel cells [12-15], or batteries [16-18]; however, all these approaches have unresolved technical challenges that obstruct their commercialization with smart lenses [19]. Although inductive power transmission can supply high power without safety issues caused by the generated heat [20], wearing the encumbered transmitter and receiver within a certain distance is necessary. This limitation would not impede special applications, such as medical diagnostics, but would make the lenses unsuitable for everyday use. Biofuel cells can generate their own power in situ but provide insufficient power densities for most applications [12-15]. Batteries can overcome both issues, providing sufficient power to the smart lens without encumbering the wearer with power transmission equipment. However, conventional batteries contain various materials, such as organic solvents and concentrated salts, that could cause severe eye damage if leaked. Therefore, the development of safe batteries is necessary for smart lens applications. Previously, we developed an aqueous battery integrated with a contact lens that operated with an artificial tear solution acting as the electrolyte, thereby circumventing any concerns about mechanical breakage and leaking hazardous chemicals [17].

To integrate various functions into smart contact lenses, all components need to be miniaturized. The power supply components are particularly difficult to miniaturize while still supplying sufficient energy because of the limited energy density of the battery and the power transmission efficiency of the receiver. Generally, batteries can be charged by supplying energy

from external power sources through wired connections or wireless transmissions. Although the wired connection is the most straightforward method, it is often impractical to make the good electrical connection needed between a small, soft electrical pad on a contact lens and an external probe. Maintaining the chemical stability of an electrical connection in fluidic media can also disrupt a direct connection. Alternatively, wireless power transmission can charge the battery while the contact lens is stored in its storage case. However, the receiving coil and control unit will occupy a large space in the contact lens.

To resolve these challenges, power from a biofuel cell could instead charge the battery without external electrical power sources, with the battery and biofuel cell integrated as individual components in the contact lens. Ideally, the battery and biofuel cell would be combined into a single component to save space in the contact lens, with the cathode and anode charged via products from enzymatic reactions in a charging solution. Since the selectively immobilized enzymes enable no membrane miniaturization, simplifying the cell configuration [21]. Our previous study also indicated that the battery could operate in an aqueous biofuel solution, potentially allowing the battery to be combined with a biofuel cell. Unlike biofuel cells that operate directly in bodily fluids, a battery combined with a biofuel cell could charge while in a contact lens case filled with a highly concentrated biofuel solution. The higher fuel concentration guarantees a high power supply to the battery from the high catalytic activity of enzymes. The battery could then be discharged at high power when needed, unlike biofuel cells that cannot store energy. Thus, combining a battery with a biofuel cell could supply higher power than individual biofuel cells powered by tears, which contain lower biofuel concentrations. Recently self-charging batteries have been developed, but these have only demonstrated self-charging of the cathode, not the anode [22]. Additionally, utilizing this self-charging mechanism could be difficult for smart contact lenses because of the air-permeable system of the battery that contains a high concentration of salts in the electrolyte. Alternatively,

oxidizing or reducing agents can be applied to charge the battery, however, their reactions are not selectively induced on the cathode or anode.

Herein, we develop our above-proposed battery design combined with enzymes, which could be charged by enzymatic reactions (i.e., bio-charging) without needing an external electrical power supply. Copper hexacyanoferrate (CuHCFe) was used for the cathode combined with the glucose oxidase enzyme (GOx). CuHCFe was oxidized (i.e., charged) by hydrogen peroxide (H_2O_2) produced by GOx with glucose in a charging solution. Polypyrrole (PPy) was used for the anode, which was reduced (i.e., charged) in the charging solution by its self-reduction ability. The cathode and anode were fabricated on a porous paper substrate to enhance the flexibility and strength of the electrodes, with the battery embedded into a contact lens. The contact lens battery was bio-charged in the glucose-based charging solution to simulate the storage of the contact lens charging at night, before being discharged in an artificial tear solution to simulate the contact lens' use in the daytime; thus, this approach simulated the cycle of contact lens usage. The cyclic performance of bio-charging was characterized, and electrical charging and discharging of the contact lens battery demonstrated the battery's general operation.

2. Results and discussion

2.1. Concept and fabrication

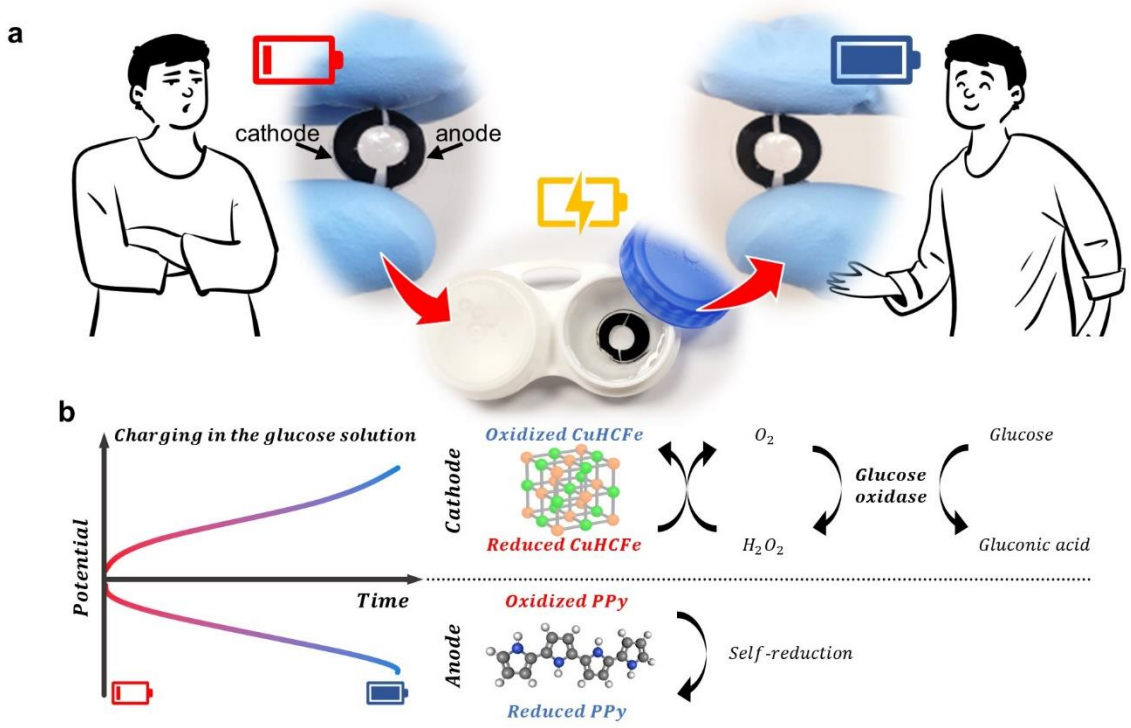

Fig. 1. (a) Illustration of bio-charging of a battery in a contact lens case. (b) Mechanism of bio-charging battery: enzymatic reaction of GOx with glucose for charging cathode and self-reduction behavior of conducting polymer for charging anode.

Fig. 1 illustrates the working principle of bio-charging of the tear-based battery and its practical usage in a smart contact lens. The battery discharges while supplying power to a smart contact lens and then is charged while the contact lens is stored in a case with a charging solution, as shown in Fig. 1a. Thus, the battery can be charged by simple immersion in the charging solution without requiring external electrical power. The CuHCFe cathode was coated with a layer of GOx and charged by immersion in a glucose solution. The GOx oxidizes glucose to gluconic acid while simultaneously reducing oxygen to H_2O_2 [23-26]. The H_2O_2 then works as an oxidizing agent of CuHCFe, and this reaction charges the cathode. Meanwhile, the anode charges through the self-reduction ability of PPy (Fig. 1b), with the oxidized PPy reduced by the nucleophilic attack of hydroxide ions [27-30]. Even low concentrations of hydroxide ions present in neutral solutions can cause this self-reduction. The discharging mechanism of the

battery is the cation intercalation of CuHCFe at the cathode and the anion coordination to PPy at the anode. The chemical reaction equations for charging and discharging are presented in Supplementary information.

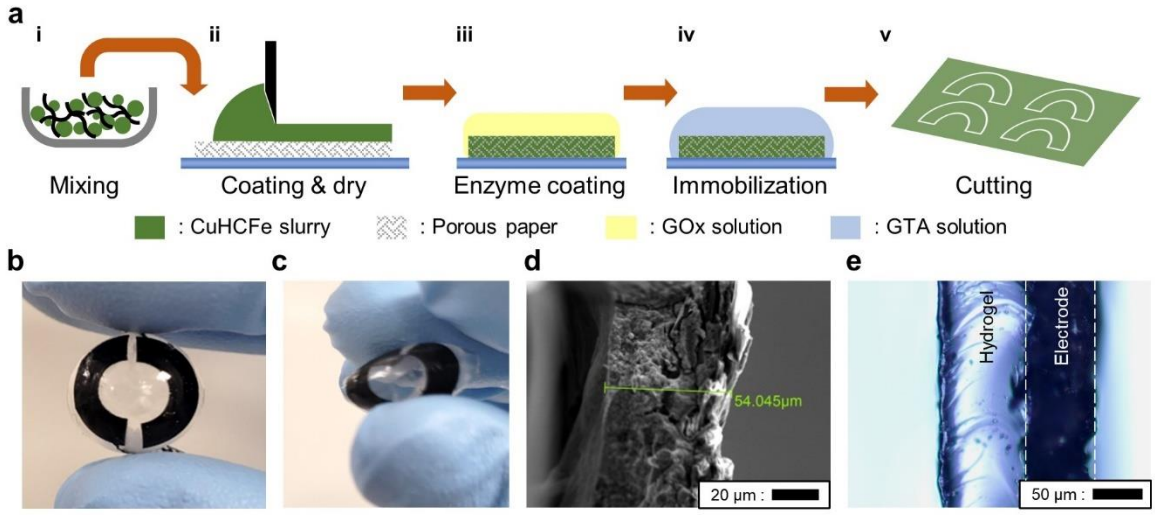

Fig. 2. (a) Schematic of electrode fabrication method. (b) Battery embedded into a soft contact lens. (c) Flexibility of the battery. (d) Cross-sectional scanning microscope image of CuHCFe electrode. (e) Cross-sectional optical microscope image of the battery embedded in a soft contact lens.

Fig. 2a illustrates the fabrication of the contact lens batteries combined with the enzyme. Porous paper (lens cleaning paper, Whatman) was used as a substrate for the electrodes to enhance their mechanical strength and flexibility. The thickness and microscopic structure of the porous paper were measured by a caliper and an optical microscope, respectively (Supplementary Fig. 3). In addition, the porous paper allowed easy handling of the free-standing film of the electrodes without damaging the electrodes during integration with the contact lens. The slurry prepared for the electrodes consisted of the active material, carbon nanotubes, carbon fibers (CFs), polyvinylidene fluoride (PVDF), and *N*-methyl-2-pyrrolidone (NMP; Fig. 2a-i), and was coated onto the porous paper (Fig. 2a-ii). The CFs were added as

additional conductive materials to improve the electrical conductivity of the electrodes. The sheet resistances of the cathode and anode were 55.9 Ω/sq and 11.6- Ω/sq, respectively (conductivity measurements are shown in Supplementary information: Conductivity measurement). Because PPy is a conductive polymer, the anode had better conductivity than the cathode. After drying the slurry, GOx was immobilized on the cathode by cross-linking between GOx and bovine serum albumin (BSA) using glutaraldehyde (GTA). The CuHCFe electrode was coated with a GOx solution prepared by dissolving GOx in deionized (DI) water together with BSA and polyvinyl alcohol on the CuHCFe electrode, which was then dried at room temperature in a vacuum chamber (Fig. 2a-iii). Next, the electrode was immersed in GTA solution and washed with DI water followed by drying in a vacuum chamber (Fig. 2a-iv). The electrodes were each cut into a c-shape and embedded into a contact lens made of hydrogel (Fig. 2a-v). The detailed fabrication process is described in the materials and methods section. The structural analysis of CuHCFe and PPy was conducted using the scanning electron microscope (SEM), X-ray powder diffraction (XRD), and Raman, respectively, as shown in Supplementary Fig. 4.

The field of vision and the flexibility of the contact lens battery were confirmed, as shown in Fig. 2b and 2c. Because the electrodes were placed at the outer side of the contact lens, the vision of the eye was not obstructed. The miniaturization of electrical parts for smart contact lenses allows enough space for integrating the electronics and sensors with the battery. Additionally, the contact lens was robust enough to withstand folding. The mechanical performance of the contact lens evaluated under frequent external bending showed no large differences in the battery capacities when applying the forces. The small changes in open circuit voltage (OCV) of the battery under manual deformation by fingers indicated the quick recovery of the battery after external disturbances. Detailed information on the mechanical performance tests is shown in Supplementary Fig. 5. Fig. 2d shows the cross-sectional image of the CuHCFe

electrode, demonstrating how the CuHCFe mixture was well distributed on the porous paper, forming an electrode 54 μm thick. The microscopic images of the top-side and bottom-side of the CuHCFe electrode indicate that the porous paper works as a structural material to hold the CuHCFe mixtures (Supplementary Fig. 6). It would be possible that the battery is embedded without thickening the conventional contact lenses as shown by the cross-sectional image in Fig. 2e. The electrode was fully covered by hydrogel and the overall thickness was 90 μm, which is thinner than conventional contact lenses (200 μm). The transmittance of the contact lens was evaluated using UV-vis, and the similar transmittance in the reference and the contact lens indicates satisfying transparency of the designed lens (Supplementary Fig. 7).

2.2. Test of the Half cell

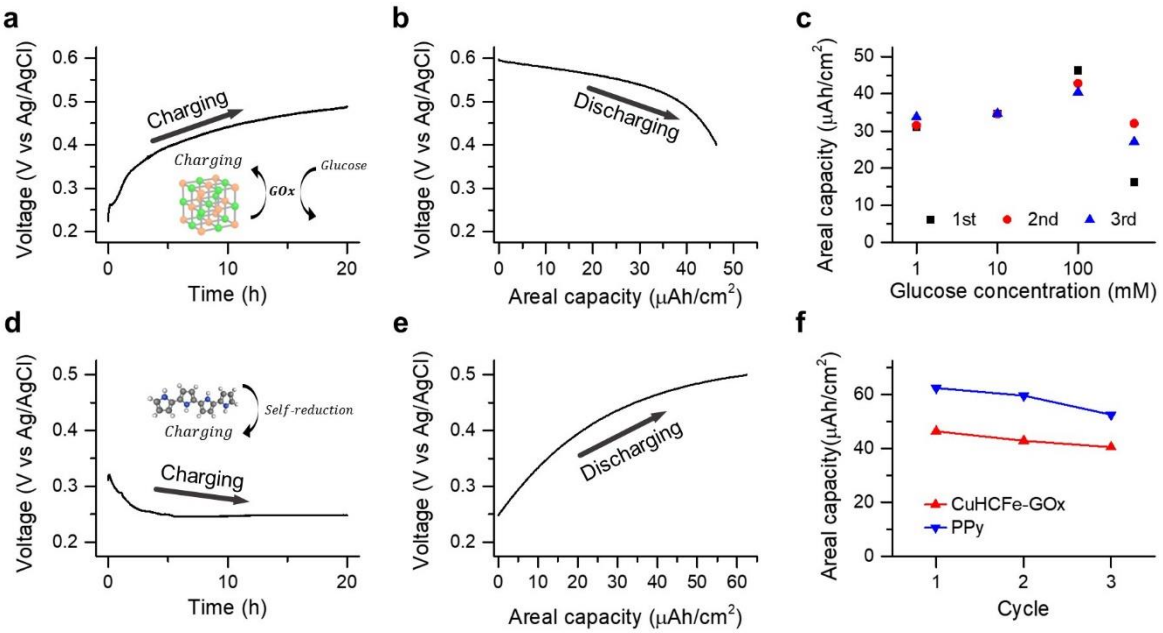

Fig. 3. Characterization of bio-charging of half-cell: (a) Charging curve of a CuHCFe electrode (cathode) in a glucose solution, (b) discharging curve of the CuHCFe electrode in an artificial tear solution, (c) concentration dependency of charging of CuHCFe electrode, (d) charging curve of a PPy electrode (anode), (e) discharging curve of the PPy electrode, (f) cyclic

performance of bio-charging of the CuHCe and PPy electrodes at the glucose concentration of 100 mM.

Half-cell tests of the cathode and anode were used to characterize the bio-charging. Fig. 3 shows the results of enzymatic oxidation of the cathode and self-reduction of the anode. The CuHCFe cathode combined with GOx was discharged (i.e., reduced) in an artificial tear solution (0.2 M NaCl and 0.15 M KCl) and then immersed in a charging solution (100 mM glucose) to charge (i.e., oxidize) the CuHCFe electrode. The open circuit voltage (OCV) of the CuHCFe electrode in the glucose solution was measured in real-time (Fig. 3a). After 20 h of charging, the CuHCFe electrode was returned to the artificial tear solution to discharge. The discharging capacity at a current of 100 μA (200 μA cm^{-2}) was 46.3 μAh cm^{-2}, as shown in Fig. 3b. The OCV of the CuHCFe electrode increased from 0.489 V (vs Ag/AgCl) to 0.605 V (vs Ag/AgCl) when switched from the charging solution to the tear solution. The formal potential of CuHCFe is related to the type of cations present and their concentration [31-33]. In general, the formal potential of CuHCFe is higher as the atomic number of the alkali metal ion is high and the concentration of the salt is high. The formal potentials of CuHCFe electrode in KCl solution showed that the formal potential of CuHCFe is higher at higher KCl concentration (the full cyclic voltammetry curves of the CuHCFe in various solutions and the calculation of the formal potential are shown in Supplementary information: Formal potential of CuHCFe). Because no salt was added to the charging solution, the potential of the CuHCFe in the charging solution was lower than in the tear solution. Fig. 3c shows the discharging capacities of the CuHCFe electrode for different concentrations of glucose in the charging solution. Higher glucose concentrations up to 100 mM led to higher discharging capacities, but higher concentrations (e.g., 500 mM) did not increase the capacity further. Up to 100 mM glucose concentration, the rate of reaction of GOx with glucose was governed by the glucose concentration of the solution, whereas above 100 mM the glucose supply from the solution to

GOx was saturated, with the rate then determined by the activity and number of enzymes present. Therefore, the CuHCFe electrode was shown to be charged by the enzymatic activity of GOx, with an optimal charging capacity provided by the 100 mM glucose solution.

The initial voltage of discharging curve of the CuHCFe in the tear solution indicated that the CuHCFe electrode was not fully charged by bio-charging because of the low electrochemical potential of H_2O_2 (the full electrochemical discharging curve of the CuHCFe is shown in Supplementary Fig. 8). The standard electrode potential of H_2O_2 is 1.78 V (vs the standard hydrogen electrode), but the actual electrochemical potential of H_2O_2 is low because of the low concentrations of H_2O_2 and protons in the solution (see details in the Supplementary information: Electrochemical potential of H_2O_2). Sodzel et al. showed that the H_2O_2 concentration produced by GOx in a 100 mM glucose solution is around 0.5 mM [34]. However, the H_2O_2 concentration in our CuHCFe electrode could not match this result because the experimental conditions, such as the density of GOx and immobilization method, are different. We believe that the H_2O_2 concentration could be similar to or even lower than these previous findings when the H_2O_2 reaches the CuHCFe electrode by diffusion. Thus, the potential of oxidation by H_2O_2 is not high enough to induce the full oxidation of CuHCFe. There are two methods to increase the charging capacity: increasing the H_2O_2 concentration and decreasing the potential of the CuHCFe electrode. The H_2O_2 concentration can be increased by optimizing the GOx activity and the potential of the CuHCFe electrode can be decreased by reducing the salt concentration. Therefore, we adjusted the glucose concentration to maximize the H_2O_2 concentration and used a DI-water-based glucose solution to minimize the salt concentration. To verify the effect of salts in the charging solution, the CuHCFe electrode was charged in an artificial-tear-based glucose solution composed of 0.2 M NaCl, 0.15 M KCl, and 100 mM glucose. This experiment showed that the CuHCFe electrode charged in the artificial-tear-based glucose solution had a lower charging capacity than when it was charged in the DI-water-based

glucose solution (Supplementary Fig. 9). In addition to the tests in glucose solutions, the CuHCFe was charged in pure DI water to verify the self-oxidation of CuHCFe (Supplementary Fig. 10). The CuHCFe electrode immersed in DI water for 20 h was then discharged, demonstrating how the discharging capacity of the CuHCFe electrode charged by self-oxidation was negligible compared with its discharging capacity when charged in a glucose solution.

The PPy anode was discharged (i.e., oxidized) in the artificial tear solution and charged in the charging solution used for the oxidation of CuHCFe. Fig. 3d shows that the real-time OCV of the PPy electrode in the charging solution gradually decreased, indicating that the PPy had been reduced. After 20 h of charging, the PPy electrode was discharged in an artificial tear solution, demonstrating a discharging capacity of 62.4 μAh cm^{-2} at a current of 100 μA (200 μA cm^{-2}), as shown in Fig. 3e. The dependence of self-reduction of PPy on the solution was confirmed by measuring its OCV in different solutions, such as various glucose concentrations, artificial tears, and DI water (Supplementary Fig. 11). The results show that the self-reduction behavior of PPy was not related to the concentration of glucose or the salt content of the solutions. Because the nucleophilic attack on PPy depends on the pH level of the solution, the PPy electrode charging could be optimized by using a more basic charging solution [30]. However, the pH level of the charging solution was adjusted to around 7 to maximize the enzymatic activity of GOx [35-37].

Bio-charging and discharging cycles of the CuHCFe and PPy electrodes were observed to verify the stability of the electrodes. Fig. 3f shows that the discharging capacities of the electrodes indicated that the enzymatic activity of GOx and the self-reduction of PPy were reversible for several cycles. The longer cycle performance of the electrodes is discussed in the following full-cell tests.

2.3. Test of the Full cell

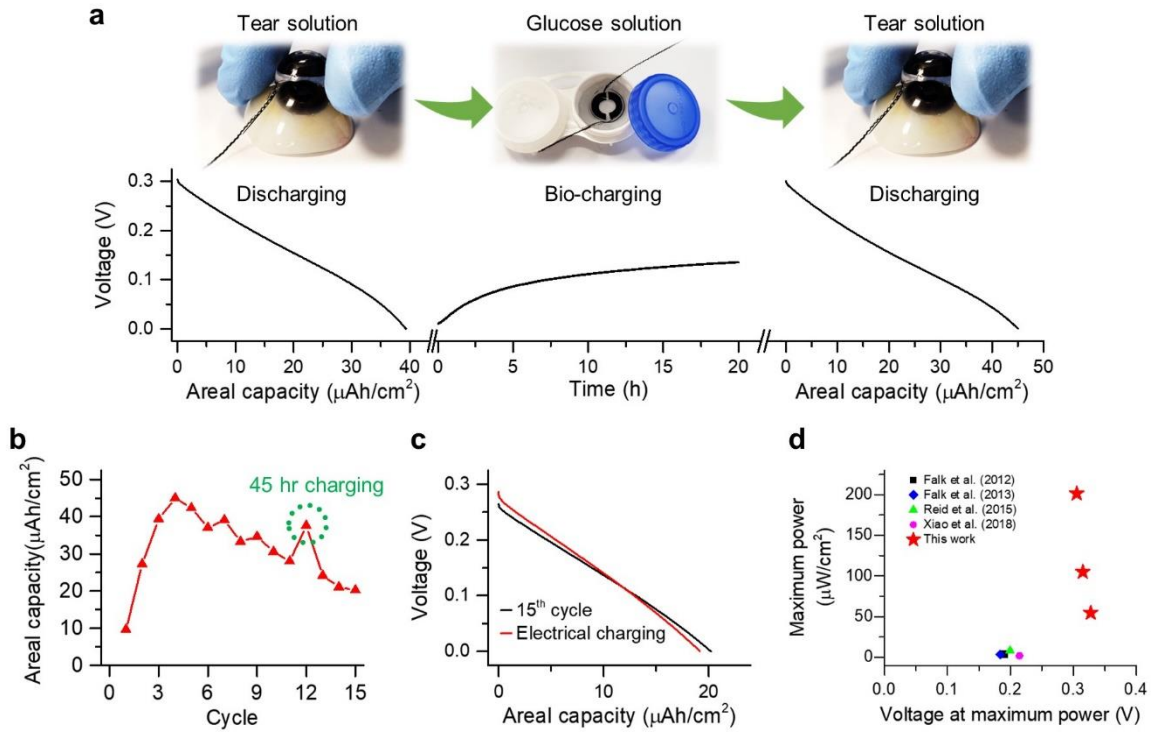

Fig. 4. Bio-charging of a battery: (a) Bio-charging and discharging cycle of the battery, (b) cyclic performance of the battery, (c) discharging curves of the battery with bio-charging and electrical charging, (d) maximum power of bio-fueled power sources for contact lenses.

After characterizing the bio-charging of the CuHCFe and PPy electrodes, the bio-charging of a full cell was characterized. The contact lens battery consisted of a CuHCFe cathode and PPy anode embedded into a contact lens made of ultraviolet-polymerized poly(hydroxyethyl methacrylate) (pHEMA), which is widely used for contact lens fabrication. Because pHEMA is polymerized at room temperature, its use avoids high-temperature processes that could destabilize the enzymes [1, 38]. Fig. 4a shows the cycles of bio-charging and discharging of the full battery cell in charging and artificial tear solutions, respectively. The battery was charged for 20 h, during which the charging process was confirmed by the battery's real-time OCV, followed by discharging at a current of 100 μA (166 μA cm^{-2}). As discussed during the

half-cell bio-charging of the CuHCFe electrode, the OCV of the battery increased when switched from the charging to the tear solution because of the salts in the charging solution because the formal potential of CuHCFe in the tear solution is higher than that in the DI-water-based glucose solution. The OCV and discharging capacity of the battery in the tear solution were 0.310 V and 27.1 μAh (45 μAh cm^{-2}), respectively.

The cycles of bio-charging and discharging were then investigated, as shown in Fig. 4b. The areal capacity of the battery increased in the initial cycles before decreasing after a few cycles. Although the latter decrease in capacity is attributable to the degradation of the enzymes, the increase in capacity during the initial cycles was not clearly understood. The hydrogel may have influenced the initial cycles of bio-charging because the half-cell not embedded in hydrogel showed no similar increase in capacity during its initial cycles. The areal capacity peaked in the full cell's fourth cycle (45 μAh cm^{-2}). Subsequently, the degradation of GOx caused a decrease in the capacity, which has previously been reported for GOx-based glucose sensors that exhibited decreased sensitivity in long-term tests [39]. We believe that 15 cycles are sufficient to demonstrate the bio-charging of the battery and that the cyclic performance of bio-charging could be improved by enhancing the biomolecules' stability. The biocompatibility of the battery was investigated by conducting the cytotoxicity test on a cultured Human Bone Osteosarcoma Epithelia cell line (U2OS cells) while charging and discharging for 24 hours. The similar observations in live and dead cells in the microscope images of live and dead cells indicated the biocompatibility of the battery, as shown in the Supplementary Fig. 12. Additionally, the lifetime of GOx can be elongated by storage below room temperature, with batteries capable of being safely refrigerated without degrading their bio-charging capacity. To demonstrate this, the bio-charging and discharging cycle of our bio-charging battery was run after being stored in a refrigerator for 12 days. The battery maintained almost the same discharging capacity as in its previous bio-charging and discharging cycles (Supplementary Fig.

13). The battery can be charged further by bio-charging for a longer time (Supplementary Fig. 14). At the 10th cycle, the battery was charged for 45 h and reached an areal capacity of 37.6 μAh cm^{-2}, which was higher than at the previous ninth cycle (28 μAh cm^{-2}) that had charged for 20 h. The self-discharging of the battery was investigated by testing the OCV of the battery in the tear-like solution after being charged under a 100 μA current for 1 hour, 5 hours, and 10 hours, respectively, as shown in Supplementary Fig. 15.

The bio-charging of the battery was compared with the electrical charging of the battery, as shown in Fig. 4c, with the battery used for bio-charging now charged by applying an electrical current. The battery was charged in the tear solution at a current of 100 μA until the voltage of the battery reached 0.3 V. The discharging curves of the bio-charged and electrically charged batteries show that the bio-charging and electrical charging produced similar outputs.

Fig. 4d shows the power of the bio-charged battery compared with biofuel cells on a contact lens [12-15]. Herein, we compared our battery with biofuel cells rather than other power sources for contact lenses because it is reasonable to compare to power sources without an external power supply. The maximum areal powers of the battery were 54 μW cm^{-2}, 105 μW cm^{-2}, and 201 μW cm^{-2} at discharging currents of 166 μA cm^{-2}, 332 μA cm^{-2}, and 664 μA cm^{-2}, respectively (the discharging curves are shown in Supplementary Fig. 16). Recently, biofuel cells for epidermal applications have been demonstrated that can supply 3.6 mW cm^{-2} [40]. However, when the biofuel cells were integrated with contact lenses, the biofuel cells could not achieve high maximum areal power because of the low biofuel concentration in the tear solution. Although our battery can supply higher power than the reported biofuel cells for smart contact lenses, the output power of the battery will need to be improved because it is still insufficient to operate electronics. For our proof-of-concept bio-charging battery, the enzymatic reaction of GOx and the self-reduction of PPy were used to charge the battery. Enhancing the

enzymatic reactions to produce higher concentrations of H_2O_2 and optimizing the structure of the electrodes to improve the transport of H_2O_2 from GOx to CuHCFe could increase the bio-charging ability. Furthermore, using enzymatic reactions on the anode or polymer with low formal potential and self-reduction behavior could lower the potential of the anode and increase the voltage of the battery.

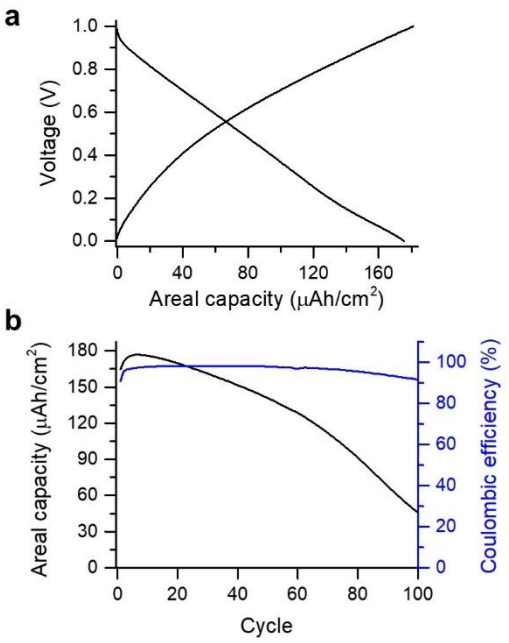

Fig. 5. Conventional battery operation: (a) Electrical charging and discharging curves of the battery with cutoff voltages of 1 V and 0 V, (b) cyclic performance of the battery.

Moreover, our contact lens battery could be used as a conventional battery as well as a bio-chargeable battery. The battery was charged by applying a current of 100 μA (166 μA cm^{-2}) with cutoff voltages of 0 V and 1 V and reached a discharging capacity of 164.9 μAh cm^{-2}, as shown in Fig. 5a. Fig. 5b shows the electrical charging and discharging cycles of the battery, which show that its capacity decreased because of mechanical stress caused by the charging and discharging detached PPy from the electrode [41]. However, this experiment demonstrates that our battery design composed of CuHCFe and PPy as the cathode and anode, respectively, is a promising enzymatic reaction-charged platform to provide voltages of up to 1 V.

3. Conclusion

We developed a contact lens battery that could be bio-charged in glucose solution for smart contact lens applications. The cathode, consisting of CuHCFe and GOx, was charged by the enzymatic reaction of GOx with glucose, while the anode was charged by the self-reduction of PPy. The proof-of-concept battery was embedded into a contact lens and had a discharging capacity of 45 μAh cm^{-2}. We confirmed that the bio-charging and discharging of the battery can be repeated for over 15 cycles and that the bio-charging of the battery is almost equivalent in output to the electrical charging of the battery. We demonstrated that the battery supplies a power of 201 μW cm^{-2}, which is much higher than that of biofuel cells for contact lenses. In addition to bio-charging, the battery can be used as conventional as well. The low output voltage of the battery could be improved by increasing the enzymatic reactivity and adopting different types of enzymes for the cathode and anode. These findings demonstrate the potential of bio-chargeable batteries for various small wearable devices, such as smart contact lenses, tooth monitoring devices, and smart patches.

4. Experimental section

4.1. Materials

Copper nitrate ($Cu(NO_3)_2$, 99%), potassium hexacyanoferrate ($K_3Fe(CN)_6$, 99%), PVDF (Mw ~534,000), NMP (99.5%), GOx (from Aspergillus niger, 100,000-250,000 units/g), BSA (heat shock fraction,98%), polyvinyl alcohol (PVA, Mw 130,000, 99%) KCl (99%), NaCl (99%), glucose (99.5%), sodium persulfate ($Na_2S_2O_8$, 98%), GTA (25w% in water), 2-hydroxyethyl methacrylate (2-HEMA, 99%) and 2-Hydroxy-2-methylpropiophenone (UV initiator, 97%)

were purchased from Sigma-Aldrich. CNT (P3-SWNT) was purchased from Carbon Solution. Pyrrole (99%) was purchased from Energy chemical. DI water was obtained from the water purifier (Direct-Q 3 UV).

4.2. Battery fabrication

Preparations of CuHCFe and PPy powders and the fabrication process of contact lenses were based on previous papers [17, 42, 43]. Briefly, 120 ml of 40 mM $Cu(NO_3)_2$ and 120 ml of 20 mM $K_3Fe(CN)_6$ were added dropwise to 60 ml of DI water at 40 °C with stirring. Precipitated CuHCFe remained in the beaker without stirring for 24 h and was purified by centrifuging and redispersing in DI water. And then, CuHCFe powders were dried in a vacuum oven. For PPy synthesis, 50 ml of 0.6 M $Na_2S_2O_8$ was added dropwise to 150 ml of 0.2 M pyrrole at 0 °C with stirring. PPy was separated from the solution by vacuum filtration and washed with DI water several times. PPy powders were redispersed in isopropyl alcohol and cut into small pieces using a hand homogenizer (3000, Dremel) because fleshly synthesized PPy contained large powders. PPy powders were obtained by centrifuge and vacuum dry processes. Slurries were prepared by mixing active material (CuHCFe or PPy), CNT, CF, PVDF, and NMP in a ratio of 8:1:3:1:80 using a mixer (AR-100, Thinky). The porous paper (lens cleaning paper, Whatman) was placed on a glass substrate and coated with the slurries using a doctor blade. The slurries were dried in a vacuum oven at 40 °C for 24 h. For the cathode, GOx was immobilized on the CuHCFe electrode. GOx and BSA were dissolved in 2 w% PVA solution, with a mass ratio of 1:0.5:10. The GOx solution was coated on the CuHCFe electrode with an areal mass loading of 1 mg cm^{-2} of GOx. The CuHCFe electrode was dried in a vacuum chamber at room temperature and a diluted GTA solution (2.5w%) was dropped on the electrode with an areal mass of 10 mg cm^{-2}. After incubating for 1 h at room temperature, the electrode was washed with DI water and dried in the vacuum chamber at room temperature. The CuHCFe and PPy

electrodes were cut into a c-shape with an inner diameter of 8 mm and an outer diameter of 16 mm. Carbon wires were connected to the electrodes using carbon slurry made by mixing carbon black, PVDF, and NMP. And then, the electrodes were embedded into a soft contact lens. The 2-HEMA-based hydrogel was polymerized using a UV-initiator with molds. A 15 mm diameter mold was used because it is the size of conventional contact lenses. The diameter electrodes were larger than the diameter of the mold to fit the film to the hemisphere.

4.3. Electrochemical measurement

For half-cell tests, a three-electrode system was built with the working electrode of CuHCFe or PPy, the reference electrode of Ag/AgCl in 4 M KCl, and the counter electrode of activated carbon. The artificial tear solution composed of 0.2 M NaCl and 0.15 M KCl was used for discharging and the 0.1 M glucose solution was used for charging. All electrochemical measurement was conducted by potentiostat/galvanostat (VSP-300, BioLogic). The cathode and anode were discharged at a current of 100 μA and stopped at voltages of 0.4 V (vs Ag/AgCl) and 0.5 V (vs Ag/AgCl), respectively. And then, the electrodes were washed with DI water using a wash bottle and charged in the glucose solution for 20 h at a temperature of 36.5 °C. For full cell tests, two electrode system was built with the working electrode of CuHCFe and the counter and reference electrodes of PPy. The battery was discharged at a current of 100 μA and stopped at a voltage of 0 V. After washing with DI water, the battery was charged in the glucose solution for 24 h at a temperature of 36.5 °C.

CRediT authorship contribution statemen

J.Y., Z.L., X.M., X.L, J.L., W.Z. and S.W.L. conceived the research. J.Y. designed and performed the experiments, characterization of the materials and analyzed the data. Z.L. performed the experiments, characterization of the materials, and cytotoxicity test of the battery.

X.M. and W.Z. contributed on the cytotoxicity test of the battery. X.L and J.L assisted in the characterization of the materials. J.Y. wrote the manuscript and all authors reviewed and revised the manuscript.

Declaration of Competing Interest

The authors declare that they have no known competing financial interests or personal relationships that could have appeared to influence the work reported in this paper.

Data availability

Data will be made available on request.

Acknowledgments

S.W.L. acknowledges the support by the National Research Foundation, Prime Minister's Office, Singapore under its NRF-ANR Joint Programme (NRF2019-NRF-ANR052 KineHarvest). W.Z. acknowledges the support by the Singapore Ministry of Education (MOE) (W. Zhao, RG112/20, and RG95/21) and the NTU Start-up Grant (W. Zhao).

Appendix A. Supplementary material

Supplementary data associated with this article can be found in the online version at.

References

[1] Y. Zhu, S. Li, J. Li, N. Falcone, Q. Cui, S. Shah, M.C. Hartel, N. Yu, P. Young, N.R. de Barros, Lab-on-a-Contact Lens: Recent Advances and Future Opportunities in Diagnostics and Therapeutics, Adv. Mater., (2022) 2108389.
[2] A. Khaldi, E. Daniel, L. Massin, C. Kärnfelt, F. Ferranti, C. Lahuec, F. Seguin, V. Nourrit, J.-L. De Bougrenet de la Tocnaye, A laser emitting contact lens for eye tracking, Scientific Reports, 10 (2020) 1-8.
[3] D.H. Keum, S.-K. Kim, J. Koo, G.-H. Lee, C. Jeon, J.W. Mok, B.H. Mun, K.J. Lee, E. Kamrani, C.-K. Joo, Wireless smart contact lens for diabetic diagnosis and therapy, Science advances, 6 (2020) eaba3252.

[4] J. Mun, T.Y. Kim, D. Myung, S.K. Hahn, Smart contact lens containing hyaluronate–rose bengal conjugate for biophotonic myopia vision correction, Biomaterials Science, 10 (2022) 4997-5005.
[5] J. Kim, E. Cha, J.U. Park, Recent advances in smart contact lenses, Advanced Materials Technologies, 5 (2020) 1900728.
[6] M. Kim, Y. Kim, J. Yun, C. Gao, H.-W. Lee, S.W. Lee, An electrochromic alarm system for smart contact lenses, Sensors and Actuators B: Chemical, 322 (2020) 128601.
[7] M. Ku, J. Kim, J.-E. Won, W. Kang, Y.-G. Park, J. Park, J.-H. Lee, J. Cheon, H.H. Lee, J.-U. Park, Smart, soft contact lens for wireless immunosensing of cortisol, Science advances, 6 (2020) eabb2891.
[8] A. Vasquez Quintero, R. Arai, Y. Yamazaki, T. Sato, H. De Smet, Near-field communication powered hydrogel-based smart contact lens, Advanced Materials Technologies, 5 (2020) 2000702.
[9] M. Yuan, R. Das, E. McGlynn, R. Ghannam, Q.H. Abbasi, H. Heidari, Wireless communication and power harvesting in wearable contact lens sensors, IEEE Sens. J., 21 (2021) 12484-12497.
[10] G.H. Lee, C. Jeon, J.W. Mok, S. Shin, S.K. Kim, H.H. Han, S.J. Kim, S.H. Hong, H. Kim, C.K. Joo, Smart Wireless Near-Infrared Light Emitting Contact Lens for the Treatment of Diabetic Retinopathy, Advanced Science, 9 (2022) 2103254.
[11] J. Park, D.B. Ahn, J. Kim, E. Cha, B.-S. Bae, S.-Y. Lee, J.-U. Park, Printing of wirelessly rechargeable solid-state supercapacitors for soft, smart contact lenses with continuous operations, Science Advances, 5 (2019) eaay0764.
[12] M. Falk, V. Andoralov, Z. Blum, J. Sotres, D.B. Suyatin, T. Ruzgas, T. Arnebrant, S. Shleev, Biofuel cell as a power source for electronic contact lenses, Biosens. Bioelectron., 37 (2012) 38-45.
[13] M. Falk, V. Andoralov, M. Silow, M.D. Toscano, S. Shleev, Miniature biofuel cell as a potential power source for glucose-sensing contact lenses, Anal. Chem., 85 (2013) 6342-6348.
[14] R.C. Reid, S.D. Minteer, B.K. Gale, Contact lens biofuel cell tested in a synthetic tear solution, Biosens. Bioelectron., 68 (2015) 142-148.
[15] X. Xiao, T. Siepenkoetter, P.O. Conghaile, D.n. Leech, E. Magner, Nanoporous gold-based biofuel cells on contact lenses, ACS applied materials & interfaces, 10 (2018) 7107-7116.
[16] C. Jeon, J. Koo, K. Lee, M. Lee, S.-K. Kim, S. Shin, S.K. Hahn, J.-Y. Sim, A smart contact lens controller IC supporting dual-mode telemetry with wireless-powered backscattering LSK and EM-radiated RF transmission using a single-loop antenna, IEEE Journal of Solid-State Circuits, 55 (2019) 856-867.
[17] J. Yun, Y. Zeng, M. Kim, C. Gao, Y. Kim, L. Lu, T.T.-H. Kim, W. Zhao, T.-H. Bae, S.W. Lee, Tear-Based Aqueous Batteries for Smart Contact Lenses Enabled by Prussian Blue Analogue Nanocomposites, Nano Lett., 21 (2021) 1659-1665.
[18] H. Lee, S. Kim, K.-B. Kim, J.-W. Choi, Scalable fabrication of flexible thin-film batteries for smart lens applications, Nano Energy, 53 (2018) 225-231.
[19] H. Mirzajani, F. Mirlou, E. Istif, R. Singh, L. Beker, Powering smart contact lenses for continuous health monitoring: Recent advancements and future challenges, Biosens. Bioelectron., 197 (2022) 113761.
[20] S.-K. Kim et al., "Bimetallic Nanocatalysts Immobilized in Nanoporous Hydrogels for Long-Term Robust Continuous Glucose Monitoring of Smart Contact Lens," Advanced Materials, vol. 34, no. 18, p. 2110536, 2022.
[21] X. Xiao, "The direct use of enzymatic biofuel cells as functional bioelectronics," eScience, vol. 2, no. 1, pp. 1-9, 2022/01/01/ 2022.
[22] Y. Zhang, F. Wan, S. Huang, S. Wang, Z. Niu, J. Chen, A chemically self-charging aqueous zinc-ion battery, Nature communications, 11 (2020) 1-10.
[23] R. Wilson, A. Turner, Glucose oxidase: an ideal enzyme, Biosens. Bioelectron., 7 (1992) 165-185.
[24] T. Kuila, S. Bose, P. Khanra, A.K. Mishra, N.H. Kim, J.H. Lee, Recent advances in graphene-based biosensors, Biosens. Bioelectron., 26 (2011) 4637-4648.
[25] T. Tzanov, S. A. Costa, G. M. Gübitz, and A. Cavaco-Paulo, "Hydrogen peroxide generation with immobilized glucose oxidase for textile bleaching," Journal of Biotechnology, vol. 93, no. 1, pp. 87-94, 2002/01/31/ 2002.
[26] J. A. Bauer, M. Zámocká, J. Majtán, and V. Bauerová-Hlinková, "Glucose Oxidase, an Enzyme "Ferrari": Its Structure, Function, Production and Properties in the Light of Various Industrial and Biotechnological Applications," (in eng), Biomolecules, vol. 12, no. 3, Mar 19 2022.
[27] P. Novák, O. Inganäs, Self-Discharge Rate of the Polypyrrole-Polyethylene Oxide Composite Electrode, J. Electrochem. Soc., 135 (1988) 2485.
[28] H. Olsson, M. Strømme, L. Nyholm, M. Sjödin, Activation barriers provide insight into the mechanism of self-discharge in polypyrrole, The Journal of Physical Chemistry C, 118 (2014) 29643-29649.
[29] H. Olsson, E.J. Berg, M. Strømme, M. Sjödin, Self-discharge in positively charged polypyrrole–cellulose composite electrodes, Electrochem. Commun., 50 (2015) 43-46.
[30] H. Olsson, Z. Qiu, M. Strömme, M. Sjödin, Parallel mechanisms of polypyrrole self-discharge in aqueous media, PCCP, 17 (2015) 11014-11019.

[31] H. Düssel, A. Dostal, F. Scholz, Hexacyanoferrate-based composite ion-sensitive electrodes for voltammetry, Fresenius J. Anal. Chem., 355 (1996) 21-28.
[32] C.D. Wessells, S.V. Peddada, M.T. McDowell, R.A. Huggins, Y. Cui, The effect of insertion species on nanostructured open framework hexacyanoferrate battery electrodes, J. Electrochem. Soc., 159 (2011) A98.
[33] R.Y. Wang, B. Shyam, K.H. Stone, J.N. Weker, M. Pasta, H.W. Lee, M.F. Toney, Y. Cui, Reversible multivalent (monovalent, divalent, trivalent) ion insertion in open framework materials, Advanced Energy Materials, 5 (2015) 1401869.
[34] D. Sodzel, V. Khranovskyy, V. Beni, A.P. Turner, R. Viter, M.O. Eriksson, P.-O. Holtz, J.-M. Janot, M. Bechelany, S. Balme, Continuous sensing of hydrogen peroxide and glucose via quenching of the UV and visible luminescence of ZnO nanoparticles, Microchimica Acta, 182 (2015) 1819-1826.
[35] H.J. Bright, M. Appleby, The pH dependence of the individual steps in the glucose oxidase reaction, J. Biol. Chem., 244 (1969) 3625-3634.
[36] Y. Zhang, S. Tsitkov, H. Hess, Proximity does not contribute to activity enhancement in the glucose oxidase–horseradish peroxidase cascade, Nature communications, 7 (2016) 1-9.
[37] H. Zhang, X. Liang, L. Han, F. Li, “Non-Naked” Gold with Glucose Oxidase-Like Activity: A Nanozyme for Tandem Catalysis, Small, 14 (2018) 1803256.
[38] A. Childs, H. Li, D.M. Lewittes, B. Dong, W. Liu, X. Shu, C. Sun, H.F. Zhang, Fabricating customized hydrogel contact lens, Scientific reports, 6 (2016) 1-9.
[39] X. Guo, B. Liang, J. Jian, Y. Zhang, X. Ye, Glucose biosensor based on a platinum electrode modified with rhodium nanoparticles and with glucose oxidase immobilized on gold nanoparticles, Microchimica Acta, 181 (2014) 519-525.
[40] Y. Yu, J. Nassar, C. Xu, J. Min, Y. Yang, A. Dai, R. Doshi, A. Huang, Y. Song, R. Gehlhar, Biofuel-powered soft electronic skin with multiplexed and wireless sensing for human-machine interfaces, Science robotics, 5 (2020) eaaz7946.
[41] Y. Liu, Q. Gan, S. Baig, E. Smela, Improving PPy adhesion by surface roughening, The Journal of Physical Chemistry C, 111 (2007) 11329-11338.
[42] M. Pasta, C.D. Wessells, R.A. Huggins, Y. Cui, A high-rate and long cycle life aqueous electrolyte battery for grid-scale energy storage, Nature communications, 3 (2012) 1-7.
[43] C. Gao, Y. Liu, B. Chen, J. Yun, E. Feng, Y. Kim, M. Kim, A. Choi, H.W. Lee, S.W. Lee, Efficient Low-Grade Heat Harvesting Enabled by Tuning the Hydration Entropy in an Electrochemical System, Adv. Mater., 33 (2021) 2004717.